Chapter

# 3

# Gas Transport Through Thermally Rearranged Nanocomposite Membranes

Contents

# Chapter - 3

# *Gas Transport Through Thermally Rearranged Nanocomposite Membranes*

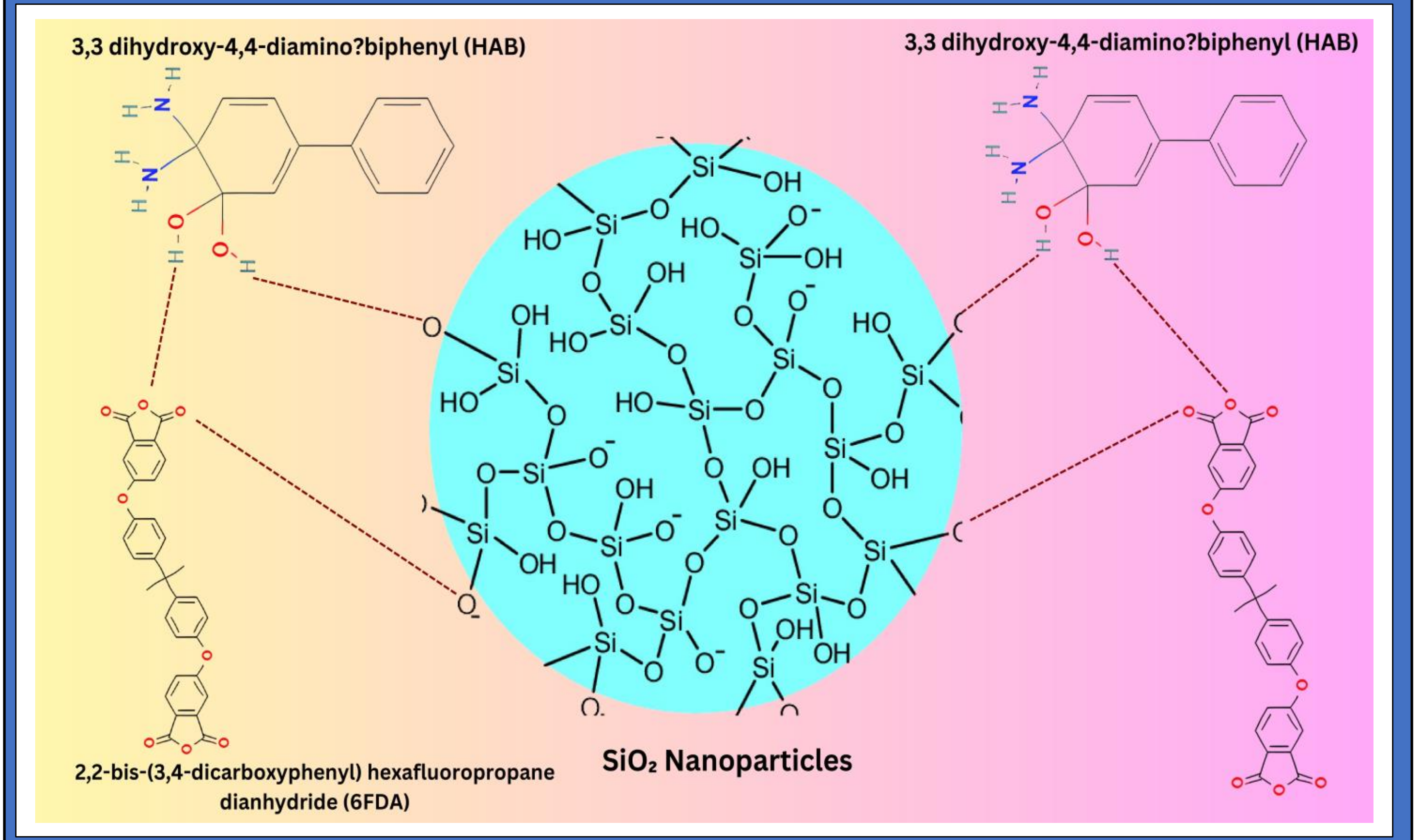

Nanocomposite membranes are a class of innovative filtering materials consisting of nanofillers embedded in a polymeric or inorganic oxide matrix that functionalizes the membrane. Thermally rearranged (TR) polymers have a good compostie of selectivity and permeability. The thermal rearrangement of polyimides of ortho-positioned functional group membranes improves the gas permselectivity properties of the polyimide precursor. This chapter, describes the synthesis of HAB-6FDA polyimide from 3,3 dihydroxy-4,4-diamino-biphenyl (HAB) and 2,2-bis-(3,4-dicarboxyphenyl) hexafluoropropane dianhydride (6FDA) by chemical imidization. A samples was modified from a pure polymer nanocomposite by incorporate of silica nanoparticle. A modification was carried out by thermal rearrangement treatment at temperatures of 350 °C, 400 °C, and 450 °C. The thermal properties of these membranes were characterized by DSC, FTIR, opacity experiment. Permeability decreases with an increase in the kinetic diameter of gasses, which is normal behaviour for glassy polymers. The composition of silica nanoparticles changes the permeability of the membrane. The combined effect of silica nanoparticles and thermal rearrangement of the HAB-6FDA membrane has shown an excellent performance. The thermal rearrangement with nanocomposite shows a significant impact on a larger effect on permeation for lighter gases, i.e. $H_2$, $CO_2$, and $O_2$, compared with $N_2$ and $CH_4$. Particularly for $H_2/CH_4$ gas pair, it lies over Robeson's 2008 upper bound limit, which fits the composition in the novel class for the gas separation membranes.

## 3.1 Introduction

Polyimide materials have shown significant potential in the field of membrane gas separation due to their ability to achieve high selectivities and low permeabilities in challenging environments [1]. As of later, Guo et al. [1] observed another group of gas separation of membranes and thermally rearranged (TR) polymers, obtained from the precursor polyimides of ortho-positioned hydroxyl groups. The thermal rearrangement of ortho-functionalized polyimides (PIs) or polyamides (PAs) may produce macromolecules that are more rigid and planar compared to the three-dimensional twisted chains of PIs [2]. This family of macromolecules is known as thermally rearranged (TR) polymers and was first described by Park et al. [3] The large torsional energy barrier against rotation between the phenylene-heterocyclic rings is what causes the microporous character. The mixture of a compact membrane containing TR polymers exhibits a notable combination of selectivity and permeability, as previously shown by Robeson's 1991 and 2008 studies, which established an upper limit for $H_2/CH_4$ separation [4]. It has been shown that gas permeabilities exhibit a significant increase after heat treatment, despite the expectation of a comparable polybenzoxazole (PBO) structure in both scenarios. The TR polymers, derived from poly(hydroxide) and ortho-acetic acid groups, have been shown in Scheme 1 to include a synthetically imidized polyimide. Furthermore, it has been shown that gas permeabilities exhibit a significant increase after heat treatment, despite the expectation of a comparable polybenzoxazole (PBO) structure.

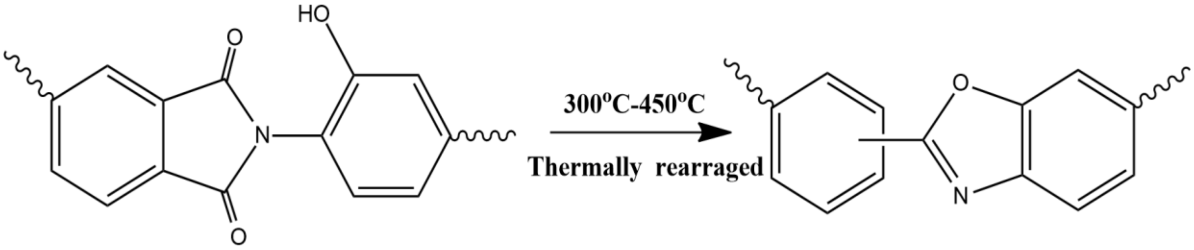

**Scheme 1:** Chemical structure of polyimide with ortho-functionality after thermal rearrangement (TR)

The results reported by Swaidan et al. [5] and our study indicate that the formation of acetate groups is more extensive than that of hydroxy groups. The addition of silica nanoparticles to polyimides further enhances gas permeability after thermal rearrangement for all gases, resulting in a more pronounced effect. In the case of lighter gases like $O_2$, $H_2$, $CO_2$, as well as $CH_4$ and $N_2$, the TR-converted nanocomposite shows a more pronounced enhancement in gas permeation. Specifically, they excelled in $H_2/CH_4$ separation, achieving excellent selectivity and high permeability when used in dense membrane configurations alongside TR.

## 3.2 Materials

Aromatic diamine, specifically 3,3-dihydroxy-4,4-diamino-biphenyl (HAB), and the dianhydride 2,2-bis-(3,4-dicarboxyphenyl) hexafluoropropylene dianhydride (6FDA). Before usage, they were dried under vacuum at temperatures of 80 °C and 160 °C. N-methyl-2-pyrrolidone (NMP) was made solvent-free through vacuum distillation with calcium hydride, and the resulting solution was stored with stirring in a sealed flask for over 3 hr. Subsequently, silica nanoparticles were subjected to sonication in dimethylacetamide (DMAc) with a concentration of 10 wt% and 15 wt% for 2 hr, followed by blending with HAB-6FDA for 6–7 hr at 35 °C temperature. The mixture of nanoparticles with the polymer solution was further stirred for an additional 50–80 cal/min. The resulting solution of composite polymer was then placed in a vacuum oven at 70 °C for 48 hr in a petri dish. Afterward, the membrane was subjected to 24 hr of drying at 70 °C to remove the majority of the soluble components, followed by another 24 hr in a vacuum oven to eliminate any remaining residues and at last membrane remove from the petri dish, this whole process known as solution casting method. The TR modification, a structural arrangement has been formed within the intramolecular positions, and the gas permeability coefficients for gases such as $O_2$, $H_2$, $CH_4$, $N_2$, and $CO_2$ was measured at 35 °C for upstream pressures up to 40 psi [6].

## 3.3 Experimental Set-up

### 3.3.1 Gas Permeability System

In this Chapter, the physical and transport properties of both pure HAB-6FDA polyimide and its thermally rearranged counterparts is reported. To determine gas permeability coefficients, selectivity, and separation factors, a constant volume/variable pressure system was primarily used. This method was consistently applied to both pure HAB-6FDA polyimide and thermally rearranged polyimides composite with 10 wt% and 15 wt% of silica nanofillers [7]. In the gas permeability measurement process, gas was introduced from the upstream side with a pressure of 30 psi into the membrane, which was positioned within the permeability cell at a temperature of (35 ± 2) ºC. By using the constant volume/variable pressure system, permeability of various gases determined including $H_2$, $CH_4$, $CO_2$, $N_2$, and $O_2$ [8].

### 3.3.2 Thermal Rearrangement (TR) Process

The thermal rearrangement of membrane samples was carried out under ambient pressure conditions using a carbolite split-tube furnace. The procedure involved the following steps: a membrane sample, with an approximate area of 8.0 $cm^2$, was prepared for the rearrangement process. The membrane sample was positioned between two ceramic plates, with a stainless steel washer placed between them. To maintain an inert atmosphere around the sample during the thermal rearrangement process, a continuous flow of nitrogen gas was introduced [9]. The nitrogen gas flow rate was set at 900 ml/min, ensuring that the environment surrounding the sample remained free of reactive gases. The sample was initially heated from ambient conditions to 300 °C at a ramp rate of 5 °C/min. Once the sample reached 300 °C, it was held at this temperature for 1 hr. This step was crucial to ensure complete imidization of the sample before proceeding with the thermal rearrangement process [10]. After the imidization step, the temperature was further increased to the desired thermal rearrangement temperature, denoted as $T_2$ (350 °C, 400 °C, or 450 °C), at a ramp rate of 5 °C/min. Subsequently, the sample was maintained isothermally at the specified thermal rearrangement temperature, $T_2$, for a duration of 10 hr, represented as $T_2 = 10$ hr in the experimental procedure. It ensured that the samples underwent the necessary thermal transformations and imidization steps before the main thermal rearrangement process, providing a consistent basis for subsequent analyses and measurements [11].

## 3.4 Results and Discussions

### 3.4.1 Gas Permeability and Selectivity

The gas permeation rate can be influenced by various factors, including the type of membrane, exposed area, working temperature, membrane thickness, and more. In this work, it is clear that the properties of the membrane, such as whether it is pure HAB-6FDA polyimide or a composite or TR membrane, play a significant role in determining the gas transfer rate. Pure HAB-6FDA polyimide membranes tend to have lower gas transfer rates compared to composite and thermally rearranged polymer nanocomposite (TR PNC) membrane. Additionally, the flow rate has been influenced by other factors like the exposed area, working temperature, and membrane thickness. The TR membrane, with higher temperatures and a higher composite rate of nanofillers, exhibited slower downstream flow rates compared to pure polyimide membranes.

**(a) 350 ºC** **(b) 400 ºC** **(c) 450 ºC**

**Figure 3.1:** Images of membrane appearance after TR process at (a) 350 ºC, at (b) 400 ºC, and at (c) 450 ºC

From visual observation, the colour of pure HAB-6FDA membranes result seems to be dark yellowish, and other thermally rearranged membranes seem dark brownish or somewhat black coloured. Figure 3.1 shows images of membrane appearance after TR process at different temperature at 350 ºC, 400 ºC, and 450 ºC. Here, when we increase the TR temperature, the colour of TR membranes becomes darker. In the case of TR PNC membranes, the rate-determining step for $H_2$ diffusion involves sorption on the membranes uper surface.

Composite nanofillers can introduce resistance, which decreases as the temperature increases. The diffusion rate of gases through TR PNC membranes at 35 ºC and various upstream pressure rates for different gases. Overall, explanation highlights the complex interplay of various factors in determining gas permeation rates through different types of membranes, including pure polyimides, composites, and TR polyimides.

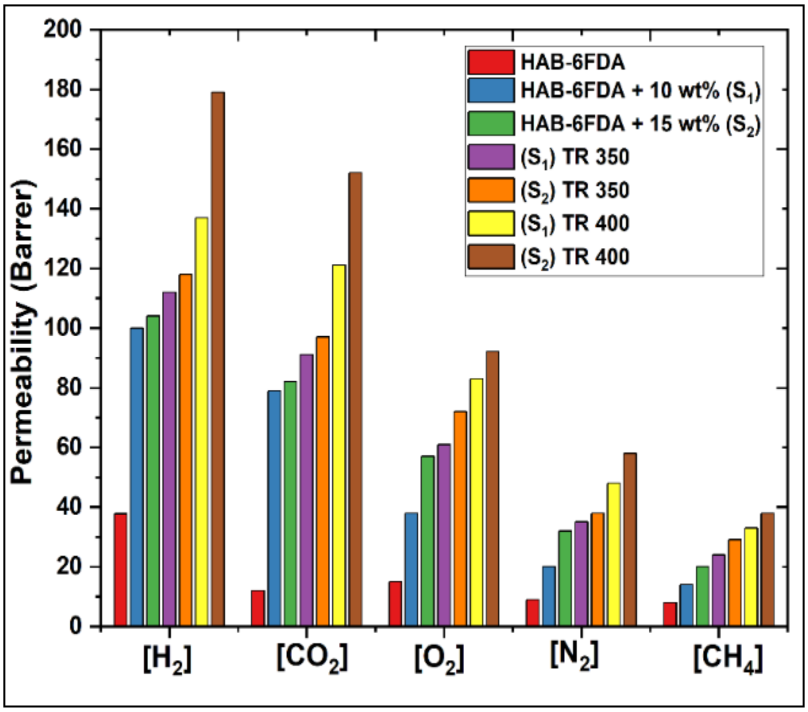

**Figure 3.2:** Permeability of pure, composite, and thermally rearranged polyimide membranes

Figures 3.2 and Figures 3.3 provide valuable insights into the gas permeability and selectivity of various composite and thermally rearranged polyimides. Figure 3.2 shows the permeability values for different gases in HAB-6FDA composite membranes with 10 wt% of silica nanofiller. It has been observed that the $H_2$ permeability is quite high, with a value of 100 Barrer. This value decreases as the kinetic diameter of the gas molecules increases, moving from $H_2$ to $CH_4$. This trend is consistent for all PNC membranes, indicating that smaller gas molecules (i.e. $H_2$) tend to permeate more easily than larger molecules (i.e. $CH_4$). Figure 3.3 shows the selectivity values for different gas pairs in HAB-6FDA polyimide composite membranes with silica nanofillers and thermally rearranged polyimides. The selectivity of $H_2/N_2$ is higher than the selectivity of $H_2/CO_2$, suggesting that $H_2$ and $N_2$ gases pass through the membrane at a similar rate, while $CO_2$ has a slightly lower permeability. The bonding strength between the nanofillers and the polymeric material plays a crucial role in improving the transfer rate and selectivity. A strong bond is necessary to withstand higher feed pressures.

Overall, these results highlight the potential for using composite and thermally rearranged polyimides with silica nanofillers for gas separation applications. The choice of nanofiller content and its dispersion within the polymeric matrix can significantly impact gas permeability and selectivity.

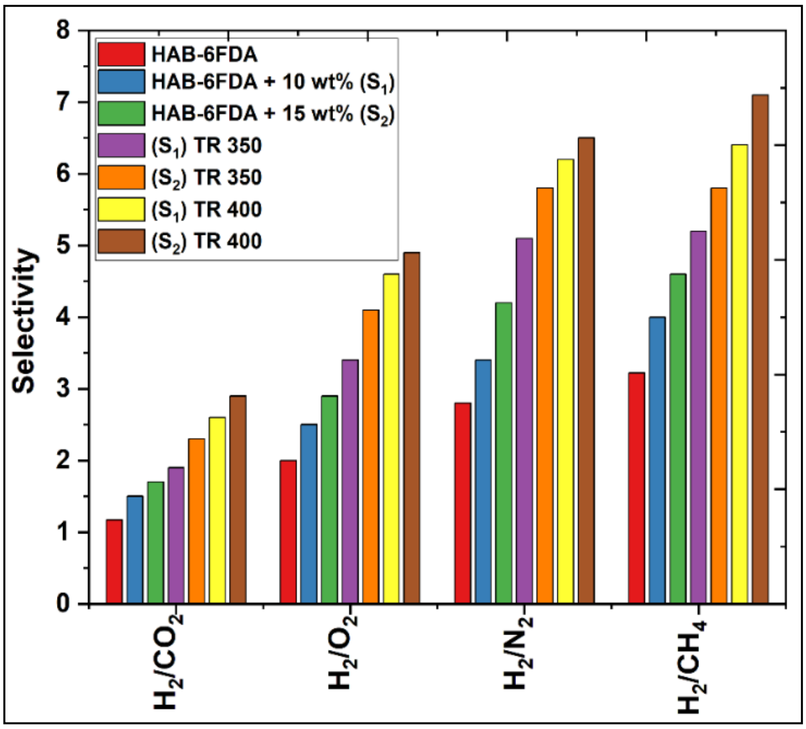

**Figure 3.3:** Selectivity of pure, composite, and thermally rearranged polyimides membranes

Figure 3.3 represents the selectivity values of HAB-6FDA polyimide, composite with silica nanofillers, and TR polyimides for $H_2/N_2$, $H_2/CO_2$, and $H_2/CH_4$ gas pairs. As seen in Figure 3.3, it is evident that the selectivity value for $H_2/N_2$ is higher than that of the $H_2/CO_2$ gas pair, indicating that a similar amount of gas passes through for $H_2$ and $CO_2$. In the Figure 3.3, the selectivity value increases for HAB-6FDA + 10 wt% ($S_1$) is 2.8 to 6.6 for ($S_2$) TR 400 in the case of $H_2/N_2$. For the $H_2/CO_2$ gas pair, the selectivity values are nearly same for all composite and TR composite membranes, indicating that hydrogen gas can be effectively separated from a mixture of $H_2$ and $CO_2$ gases.

As shown in Table 3.1, the permeability exhibits an upward trend as the weight percentage (wt%) of silica nanofillers is increased. This trend has been particularly pronounced for gas molecules with larger kinetic diameters, where the increase in permeability is more noticeable. Silica nanofillers play a crucial role in augmenting gas permeability and expanding the fractional free volume (FFV) within the polyimide composite. The permeability of pure HAB-6FDA polyimide is 37.8 Barrer. However, when this pure polyimide is combined with

10 wt% of silica nanofillers, the permeability significantly increased to 100 Barrer. Furthermore, at a silica nanofiller content of 15 wt%, the permeability reaches 104 Barrer. Silica nanofillers are instrumental in enhancing permeability by creating additional space between the polyimide chains.

**Table 3.1:** Permeability (Barrer) of different composite and thermally rearranged polyimide membranes

| **Membranes** | **$H_2$ (Barrer)** | **$CO_2$ (Barrer)** | **$O_2$ (Barrer)** | **$N_2$ (Barrer)** | **$CH_4$ (Barrer)** |
|---|---|---|---|---|---|
| **HAB-6FDA** | 37.8 | 12 | 15 | 9 | 8 |
| **HAB-6FDA+ 10 wt% ($S_1$)** | 100 | 79 | 38 | 20 | 14 |
| **HAB-6FDA+ 15 wt% ($S_2$)** | 104 | 82 | 57 | 32 | 20 |
| **($S_1$) TR 350** | 112 | 91 | 61 | 35 | 24 |
| **($S_2$) TR 350** | 118 | 97 | 72 | 38 | 29 |
| **($S_1$) TR 400** | 137 | 121 | 83 | 48 | 33 |
| **($S_2$) TR 400** | 179 | 152 | 92 | 58 | 38 |

Regarding the thermal rearrangement (TR) process with silica composite membranes, an increase in the heating rate results in increased permeability. Nonetheless, for gases like oxygen ($O_2$), nitrogen ($N_2$), and methane ($CH_4$), the permeability tends to saturate as the TR temperature increases. This saturation occurs due to the relatively larger kinetic diameters of these gas molecules compared to hydrogen ($H_2$) and carbon dioxide ($CO_2$) [12]. It is worth noting that the thermal rearrangement process primarily influences changes in the polymer structure, leaving the nature of the silica nanoparticles unaltered. However, it may cause variations in the distribution of these nanoparticles within the polymer matrix, consequently affecting permeation behaviour. As shows in the Figure 3.2, the $H_2$ permeability of the HAB-6FDA composite with 10 wt% silica nanofiller witth TR 400 observed at 179 Barrer. This value experiences a decline as we move from gases with lower kinetic diameters, such as hydrogen

($H_2$), to those with larger kinetic diameters, i.e. Methane ($CH_4$). Furthermore, when the 15 wt% nanofiller composite HAB-6FDA membrane undergoes thermal rearrangement (TR), there is a substantial increase in permeability compared to both the pure polymer membrane and the PNC membrane. This increment in permeation effect has been more pronounced for lighter gases like $H_2$, $CO_2$, and $O_2$, as observed and plotted in Figure 3.2 [13].

Silica nanofillers play a significant role in this process, as they disperse within the membrane they create additional cavities. These cavities, combined with the existing free volume, collectively contribute to the overall free volume within the membrane structure. This large free volume within the polymer matrix allows for an increased sorption capacity and provides diffusion pathways for gas molecules. The larger free volume accommodates a greater number of diffusion paths for gas molecules, facilitating their movement. Weak adhesion between the polymer and inorganic nanofiller results in nanogaps at the boundary phases, enabling gas molecules to more easily traverse these gaps [14]. Increasing the filler concentration, especially at 15 wt% silica, leads to the expansion of the inter-aggregate space between nanofiller aggregates. This additional free volume, in conjunction with the fractional free volume (FFV), enhances the passage of larger gas molecules through the membrane [15]. The trend between permeability and the selectivity of pure gases shows that selectivity increases as the conversion rate of silica nanofillers increases and TR temperature increased. Additionally, permeability decreases progressively as the transformation rate increases. It is important to note that the rate of change in selectivity is less than the transformation rate. For example, when the transformation rate increases from 57% to 78%, selectivity has been reduced by only 14%. This outcome suggests that high permeability/selectivity can be achieved by modifying the polymer through the thermal rearrangement process.

The composition of polymer membranes containing HAB-6FDA and silica nanofiller results in higher permeability than pure polyimides. However, the permeability is increased by more than four times in the case of thermally rearranged polyimides [16].

### 3.4.2 Robeson's Upper Bound Plots

Figure 3.4 shows the trade-off relationship between $H_2/CO_2$ selectivity and $H_2$ permeability. The same logarithmic scale has been used to establish the trade-off correlation between selectivity for different gas pairs and permeability, and the required upper limits are calculated. When assessing the selectivity values presented in the chart for the $H_2/CO_2$ gas pair, obtained from the corresponding data for the pure polymer membrane, there is a reduction in magnitude for the HAB-6FDA. However, the thermally rearranged HAB-6FDA membrane has increased the value. The TR results indicate a decline in the separation aspect. Robeson's upper bound plots are graphical representations used in the field of membrane based gas separation to illustrate trade-off between permeability and selectivity of membranes. Enhancing permeability (allowing more gas to pass through) may come at the expense of selectivity (the ability to distinguish between different gases). On a Robeson's upper bound plot, actual or potential membrane materials are plotted as data points. These points represent the performance of specific membranes for a particular gas separation. The trade-off between permeability and selectivity becomes evident by examining the distribution of these points relative to the upper bound line. In contrast to the other experiments, the selectivity of the PNC membrane decreases. However, the selectivity for the TR membrane improves for $H_2/CO_2$ gas pair when the temperature has been increased.

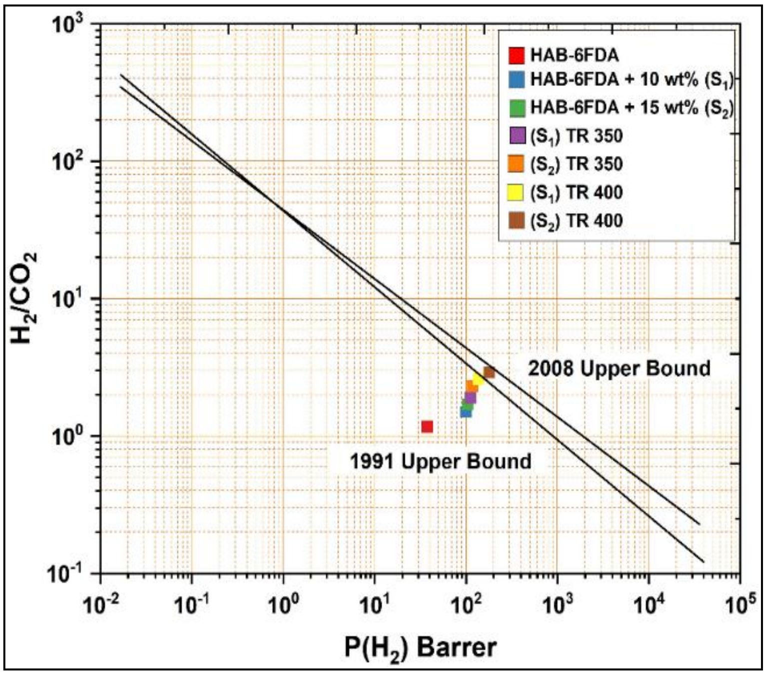

**Figure 3.4:** Robeson upper bound correlation for $H_2/CO_2$ separation

As the temperature increases, sorption capacities decreases due to reduced surface energy, while the activated gas movement increases through the openings in the polymer structure due to the thermal process.

As a result, such a membrane may effectively separate $H_2$ from $CO_2$, and selectivity is limited for mixed samples when exposed to $H_2/CO_2$. Compared to the pure polymer, TR PNC's selectivity increases, as shown in Figure 3.4.

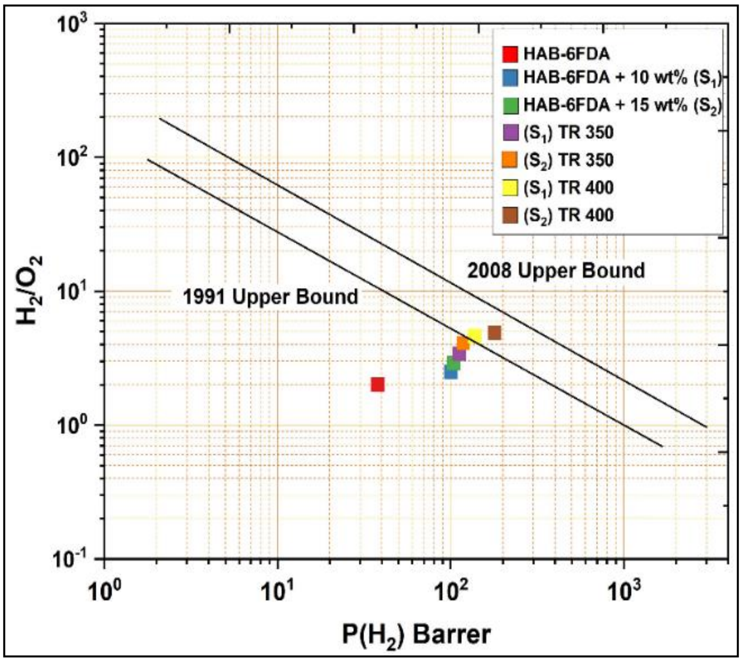

**Figure 3.5:** Robeson upper bound correlation for $H_2/O_2$ separation

The separation of $H_2$ as of $O_2$ has controlled by TR PNC and PNC membranes in more significant amounts, but it has an extraordinary effect on TR PNC as detected in Figure 3.5. The enormous outcome can be noticed for $H_2/O_2$ separation for which the materials lie on the 1991 upper bound limit in Figure 3.5. This results has potential applications in recovering hydrogen from ammonia purge gas in large-scale commercial membrane-based gas separation processes over time [17]. The separation efficiency of $H_2$, particularly when separating it from $N_2$ gas, has notably improved.

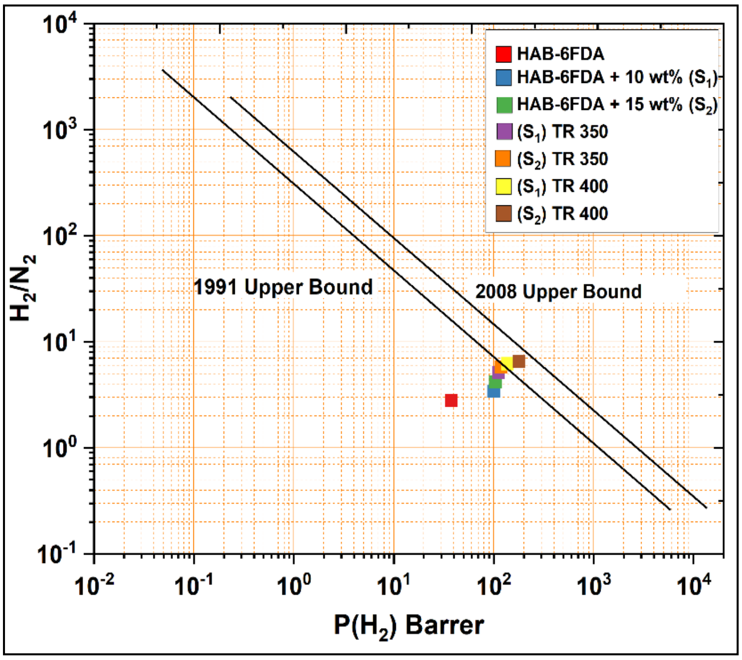

**Figure 3.6:** Robeson upper bound correlation for $H_2/N_2$ separation

The results indicate that this specific gas pair exhibits the highest selectivity compared to all other combinations. The membranes with TR process of ($S_2$) TR 400 achieves the highest level of separation [18]. Furthermore, when examining the Robeson plot for $H_2/N_2$, most of the developed composites fall within the upper bound limit set by Robeson in 1991. However, ($S_2$) TR 350, ($S_1$) TR 400, and ($S_2$) TR 400 have exceeded this upper bound limit, as shown in Figure 3.6. The selectivity of $H_2/N_2$ is improved for both silica loading and the TR process [19]. Additionally, in the upper bound plot, all the membranes are positioned below the limiting line established in 2008.

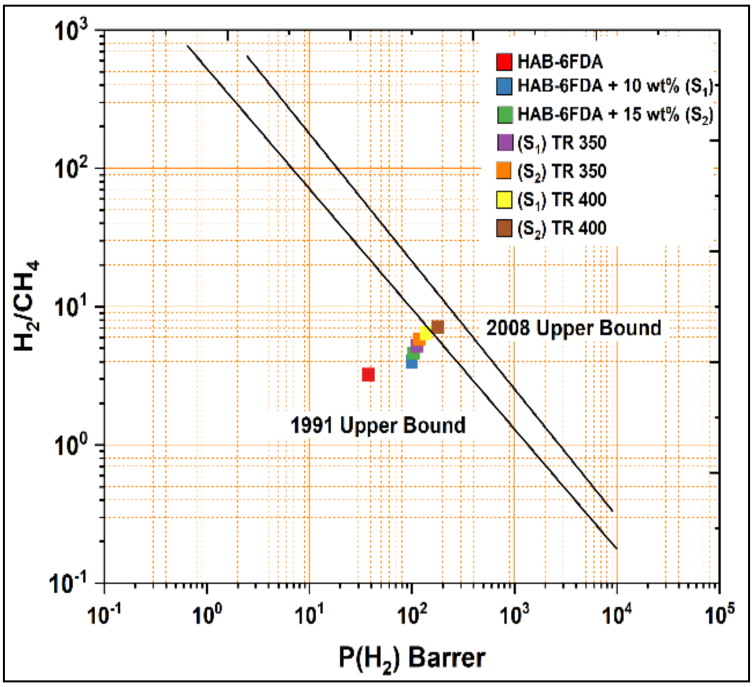

**Figure 3.7:** Robeson upper bound correlation for $H_2/CH_4$ separation

In this context, the significant separation of $H_2$ from $CH_4$ has been predominantly achieved with PNC membranes, and TR PNC membranes exhibit remarkable performance in this regard, as shown in Figure 3.7. Furthermore, TR PNC membranes can provide even purer results than PNC membranes. The selectivity of thermally rearranged nanofiller-dispersed membranes shows great promise for separating $H_2$ from methane gas streams. Even after distillation, residual $CH_4$ is usually present in $H_2$ because it has been formed during steam-reforming hydrocarbons. TR PNC membranes are capable of producing highly pure hydrogen. Therefore, the newly designed TR PNC membrane is well-suited for separating $H_2$ from syngas. The $H_2$ separation process finds applications in various industries, including petrochemical plants and gas separation units, especially those involved in hydrogen gas separation for refinery operations, oxo-chemical processes, and gas purification applications.

Traditionally, palladium has been used to produce high-purity $H_2$ gas, but it is known to have certain limitations and impurities associated with the materials used in the process [20]. In applications such as gas purification and chemical imidization, a combination of gas separation membranes has commonly used to isolate hydrogen gas. However, using nanofiller composite membranes can be economically costly. Therefore, this innovative membrane modification composition may offer a cost-effective solution for obtaining highly purified hydrogen gas with the need of silica nanofillers.

### 3.4.3 Differential Scanning Calorimetry (DSC)

The thermal properties of pure HAB-6FDA polyimides were characterized using differential scanning calorimetry (DSC) analysis, the detail parameters of instrument has been discussed in chapter 2.

The DSC analysis involved measuring the heat flow versus temperature, to determine the glass transition temperature ($T_g$) and TRIOS software was used to analyzed the raw data. The pure HAB-6FDA polymer exhibits a glass transition temperature ($T_g$) at approximately 265 ºC. In contrast, the thermally rearranged polyimides in membranes shows a higher $T_g$, around 290 ºC, than the pure polymer. As the rate of TR heating protocol and the silica nanofiller content are increased, the $T_g$ value also increased, as evident from these results [21]. This increase in $T_g$ occurs due to the composite of silica nanofillers leads to an increase in fractional free volume between the chains of the polymer. The value glass transition temperature of various samples has been shown in Table 3.2.

**Table 3.2:** Glass transition temperature ($T_g$) value of different polymers composite material and TR processed membranes

| **Material** | **Glass transition Temperature ($T_g$) (°C)** |
|---|---|
| **HAB-6FDA + TR 350** | 277 |
| **($S_1$) TR 350** | 277 |
| **($S_2$) TR 350** | 281 |
| **HAB-6FDA + TR 400** | 294 |
| **($S_1$) TR 400** | 295 |
| **($S_2$) TR 400** | 295 |

Notably, the glass transition temperature for (HAB-6FDA + 10 wt% of $SiO_2$ ) TR 400 overlaps with that of (HAB-6FDA + 15 wt% of $SiO_2$) TR 400, and (HAB-6FDA ) TR 350 overlaps with (HAB-6FDA + 10 wt% of $SiO_2$) TR 350, which is observed from Table 3.2. These results demonstrate a broad range of thermal transitions spanning from 350 ºC to 400 ºC, with calculated glass transition temperatures ranging from around 260 ºC to 295 ºC for both pure and thermally rearranged HAB-6FDA polyimides. It has been observed that ortho-functional groups in the thermally rearranged polyimides, specifically ortho-positioned hydroxy groups, contribute to better thermal stability compared to acetate groups.

## 3.5 Conclusion

The research focuses on the modification of HAB-6FDA pure polymer membranes using a chemical imidization process to transform them into ortho-functional thermally rearranged polyimides. The study incorporates data from six different sets of membranes, including results from DSC, to establish a clear relationship between the glass transition temperatures ($T_g$) of pure HAB-6FDA polymer membranes and modified thermally rearranged polyimides. The conversion process from pure HAB-6FDA to PNC membranes began at TR 300 with the addition of silica nanofillers. The highest heating level used at 450 °C. These membranes shows excellent permeability to different gases, attributed to the increase in fractional free volume. This shows the remarkable performance enhancement resulting from the composite of silica nanofillers and the thermal treatment of HAB-6FDA. Interestingly, the TR-adapted nanocomposite exhibits a more substantial increase in permeability for lighter gases like $CO_2$ and $O_2$ when compared to heavier gases like $N_2$ and $CH_4$. The presence of $SiO_2$ nanoparticles plays very important role in enhancing the transport of $H_2$ molecules within this nanocomposite polyimide. Moreover, as the silica content increases, it results in a greater amount of free space within the material, further contributing to improved permeability. Remarkably, some of the materials developed in this study have surpassed the upper limits established by Robeson in 1991 and 2008, demonstrating their exceptional gas separation performance. In summary, the combination of silica nanofillers and the thermal rearrangement process has led to remarkable improvements in the properties of polyimide membranes, in terms of gas permeability and selectivity. These results, supported by various analytical techniques, underscore the potential of these membrane materials for a wide range of gas separation applications.

## References:

[1] R. Guo, D. F. Sanders, Z. P. Smith, B. D. Freeman, D. R. Paul, and J. E. McGrath, Synthesis and characterization of Thermally Rearranged (TR) polymers: Influence of ortho-positioned functional groups of polyimide precursors on TR process and gas transport properties, *J. Mater. Chem. A*, **2013**, 1 (2), 262–272.

[2] B. Comesaña-Gándara, A. Hernández, J.G. de la Campa, J. de Abajo, A.E. Lozano, and Y. M. Lee, Thermally rearranged polybenzoxazoles and poly(benzoxazole-co-imide)s from ortho-hydroxyamine monomers for high performance gas separation membranes, *J. Memb. Sci.*, **2015**, 493, 329–339.

[3] H. B. Park, S. H. Han, C. H. Jung, Y. M. Lee, and A. J. Hill, Thermally rearranged (TR) polymer membranes for $CO_2$ separation, *J. Memb. Sci.*, **2010**, 359 (1–2), 11–24.

[4] H. Ahmadizadegan, S. Esmaielzadeh, Fabrication and Characterization of Novel Polyester Thin-film Nanocomposite Membranes Achieved by Functionalized $SiO_2$ Nanoparticles for Gas Separation, *Poly. Eng. and Sci.*, **2018**, 59, 237-247.

[5] R. Swaidan, X. Ma, E. Litwiller, and I. Pinnau, High pressure pure- and mixed-gas separation of $CO_2/CH_4$ by thermally-rearranged and carbon molecular sieve membranes derived from a polyimide of intrinsic microporosity, *J. Memb. Sci.,* **2013**, 447, 387–394

[6] S. H. Han, N. Misdan, S. Kim, C. M. Doherty, A. J. Hill, and Y. M. Lee, Thermally rearranged (TR) polybenzoxazole: Effects of diverse imidization routes on physical properties and gas transport behaviours, Macromolecules, **2010**, 43 (18), 7657–7667.

[7] D. F. Sanders, Z. P. Smith, Ribeiro, R. Guo, J. E. McGrath, D. R. Paul, and B. D. Freeman, Gas permeability, diffusivity and free volume of thermally rearranged polymers based on 3,3’-dihydroxy-4,4’-diamino-biphenyl (HAB) and 2,2’-bis-(3,4-dicarboxyphenyl) hexafluoropropane dianhydride (6FDA), *J. Memb. Sci.*, **2012**, 409–410, 232–241.

[8] A. K. Patel, N. K. Acharya, Thermally rearranged (TR) HAB-6FDA nanocomposite membranes for hydrogen separation, *Int. J. Hydrogen Energy*, **2020**, 45 (37), 18685–18692.

[9] D. Bikiaris, J. Prinos, M. Botev, C. Betchev, and C. Panayiotou, Blends of polymers with similar glass transition temperatures: A DMTA and DSC study, *J. Appl. Polym. Sci.*, **2004**, 93 (2), 726–735.

[10] Y. K. Vijay, N. K. Acharya, S. Wate, and D. K. Avasthi, Nanofilter for hydrogen purification, *Int. J. Hydrogen Energy*, **2003**, 28, 1015–1018.

[11] C. Mariola, M. Cara, J. Doherty, J. Anita, Hill and Young Moo Lee, Cross-Linked Thermally Rearranged Poly(benzoxazole-co-imide) Membranes for Gas Separation, *Macromolecules*, **2013**, 46 (20), 8179 - 8189.

[12] Y. K. Ong, H. Wang, and T. S. Chung, A prospective study on the application of thermally rearranged acetate-containing polyimide membranes in dehydration of biofuels via pervaporation, *Chem. Eng. Sci.,* **2012**, 79, 41–53.

[13] Y. M. Xu, N. L. Le, J. Zuo, and T. S. Chung, Aromatic polyimide and crosslinked thermally rearranged poly(benzoxazole-co-imide) membranes for isopropanol dehydration via pervaporation, *J. Memb. Sci.*, **2016**, 499, 317–325.

[14] A. C. Comer, C. P. Ribeiro, B. D. Freeman, S. Kalakkunnath, and D. S. Kalika, Dynamic relaxation characteristics of thermally rearranged aromatic polyimides, *Polymer*, **2013**, 54 (2), 891–900.

[15] A. K. Zulhairun, B. C. Ng, A. F. Ismail, R. S. Murali, and M. S. Abdullah, Production of mixed matrix hollow fiber membrane for $CO_2/CH_4$ separation, *Sep. Purif. Technol.*, **2014**, 137, 1–12.

[16] A. K. Patel, N. K. Acharya, Study of gas transport phenomenon in layered polymer nanocomposite membranes, *Trends Appl. Adv. Polym. Mater.*, **2017**, 191–206.

[17] F. Kremer, M. Tress, and E. U. Mapesa, Glassy dynamics and glass transition in nanometric layers and films: A silver lining on the horizon *J. Non. Cryst. Solids*, **2015**, 407, 277–283.

[18] N. Shamim, Y. P. Koh, S. L. Simon, and G. B. McKenna, The glass transition of trinitrotoluene (TNT) by flash DSC, *Thermochim. Acta*, **2015**, 620, 36–39.

[19] G. C. Huang, and J. K. Lee, Isothermal cure characterization of fumed silica/epoxy nanocomposites: The glass transition temperature and conversion, *Compos. Part A Appl. Sci. Manuf.*, **2010**, 41 (4), 473–479.

[20] K. D. Sitter, P. Winberg, J. D'Haen, C. Dotremont, R. Leysen, J. Martens, S. Mullens, F. H. Maurer, and I. F. Vankelecom, Silica filled poly(1-trimethylsilyl-1-propyne) nanocomposite membranes: Relation between the transport of gases and structural characteristics, *J. Memb. Sci.*, **2006**, 278 (1–2), 83–91.

[21] S. A. Habibiannejad, A. Aroujalian, A. Raisi, Pebax-1657 mixed matrix membrane containing surface modified multi-walled carbon nanotubes for gas separation, *RSC Adv.*, **2016**, 6 (83), 79563–79577.